Proceedings 10th NUMGE 2023
10th European Conference on Numerical Methods in Geotechnical Engineering
Zdravkovic L, Kontoe S, Taborda DMG, Tsiampousi A (eds)

https://doi.org/10.53243/NUMGE2023-383

Seismic behaviour of a tailings dam in Peru

C. Salvador[1], F. Robles[1], C. Romanel[1]

[1] *Pontifícia Universidade Católica do Rio de Janeiro, Department of Civil and Environmental Engineering, Rio de Janeiro, Brazil*

ABSTRACT: This paper presents a study on the seismic behaviour of an upstream tailings dam situated in the province of Arequipa, Peru. In 2013 seismic events caused cracks in the dam body, crest settlements and sand boils due to liquefaction. In this investigation, the seismic hazard assessment was determined by probabilistic methods and design earthquakes were generated complying with the risk rating recommendations for the global industry standard on tailings management. A finite element numerical analysis was performed considering the PM4Sand and PM4Silt constitutive elastoplastic models. Numerical results were presented in terms of permanent displacements and pore pressure distribution immediately after the earthquake duration, thus indicating that the Otapara tailings dam will suffer dynamic liquefaction for 1000 year return period earthquakes.

Keywords: Tailings dam; design earthquake; seismic behaviour; dynamic liquefaction

1 INTRODUCTION

Peru is located in an region of high seismic activity, with different earthquakes faulting mechanism due to interaction between the Nazca and the South American tectonic plates. Mining is a very important economic activity for the country which requires the construction of civil engineering structures, such as tailings dams, in order to store large amounts of waste materials.

In this paper, the seismic behaviour of the Otapara tailings dam is investigated with emphasis on simulation of the dynamic liquefaction of the tailings by the finite element method (FEM).

One important ingredient for FEM analysis is the elastoplastic model incorporated in numerical simulations. In the literature, there are some suggestions for dynamic liquefaction prediction of sand-like materials, such as the UBCSand model (Beaty and Byrne, 1998) and its 3D generalization UBC3D-PLM (Tsegaye, 2010) which incorporates a soil densification rule in order to predict a more realistic evolution of excess pore pressures during cyclic loading. However, this rule works consistently only in the case of symmetric loading and for stress paths that start from the isotropic axis. Also, UBC3D-PLM does not include the influence of the effective confining pressure on the cyclic resistance of the soil (Petalas and Galavi, 2013).

The SANISAND models (Dafalias and Manzari, 2004; Taiebat and Dafalias, 2008; Dafalias et al., 2016; Petalas et al., 2019; Papadimitriou et al., 2019; Petalas et al., 2020) are another class of models based on the framework of bounding surface plasticity and critical state mechanics concepts. A model referred to as SANISAND-Sf (Barrero et al., 2020) has been recently proposed to capture the post-liquefaction cyclic shear strain behaviour of sands, reflecting the physical existence of a "semifluidized (Sf) state" for very low effective mean stress reached in the post-liquefaction stage. This model introduces a new internal degradation variable that affects the plastic modulus and dilatancy within the Sf state, while leaving almost intact the response outside of it. Aside from the constants with default numerical values, SANISAND-Sf model requires the calibration of 20 model constants: 15 of them inherited from SANISAND and the remaining 5 related to the Sf state.

The PM4Sand model (Boulanger and Ziotopoulou, 2015) is a 2D plane-strain model that follows the basic framework of the stress-ratio controlled, critical state compatible, bounding-surface plasticity model for sand presented by Dafalias and Manzari (2004). The model parameters are grouped into two categories: a primary set of 3 parameters (apparent relative density D_R, shear modulus coefficient G_0, contraction rate parameter hp_0) that are most important for model calibration, and a secondary set of parameters (18 in total and optional) that may be modified from their default values in special circumstances. By changing the three primary input parameters it is possible to achieve reasonable approximations of desired behaviour including pore pressure generation and dissipation, limiting strains, and cyclic mobility. The apparent relative density D_R has the most crucial effect in the cyclic strength and also significant influence in the generation of excess pore pressures, while the shear modulus coefficient G_0 has minor influence in the cyclic strength, and it not affects the generation of excess pore pressures until a pore pressure ratio r_u of around 1.0 is reached. Since its introduction, the PM4Sand model has drawn wide

attention in geotechnical engineering practice and research communities due to its relatively easy calibration process and good agreement with field observations.

2 OTAPARA TAILINGS DAM

2.1 Location

The Otapara tailings dam is situated in the province of Arequipa, Peru, at an average elevation of 430 meters above sea level. Figure 1 indicates the location of the dam in relation to the Acarí River and the city of Otapara-Acarí.

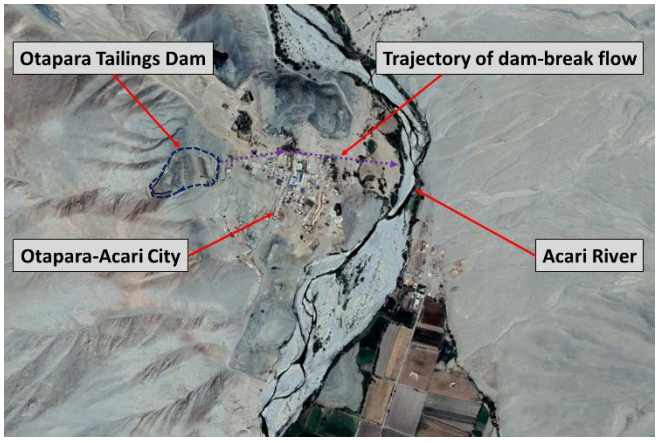

Figure 1. Otopara dam, Otapara-Acari city and trajectory of dam-break flow.

2.2 Characteristics of the tailings dam

The Otapara tailings dam consists of an embankment, built with borrow material, and subsequently raised by the upstream construction method, using cyclonic tailings released from the crest where they were deposited in a fully saturated condition with low relative density. Figure 2 shows the critical cross-section of the dam at the end of construction.

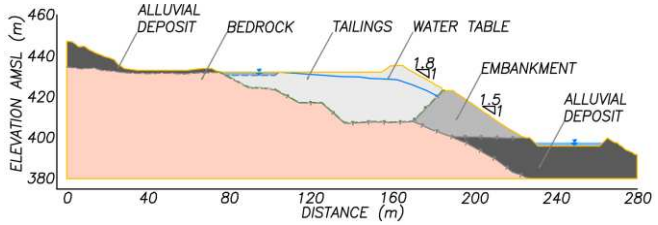

Figure 2. Critical cross-section of the Otapara dam.

The pulp-type tailings are pumped from the mining plant to the disposal pond, forming a beach. The reservoir has a waterproofing geomembrane lining at the bottom, as well as surface and deep water drainage systems and ponds for leachate treatment. According to the shear wave velocity (V_s) the reservoir bedrock is classified as a site class B (ASCE 7-16, 2017).

2.3 Field and laboratory tests

The geotechnical characterization of soils was carried out through field and laboratory tests. The field tests (58 SPT and 10 CPT) were adequately distributed over the area of interest, in order to estimate the shear strength and consistency / compaction of soils that make up the tailings deposit. In some selected samples, laboratory tests were executed to determine the soil classification, according to the Unified Soil Classification System (USCS), as well as the wet density and specific gravity. To evaluate the resistance properties, direct shear tests were carried out on samples of coarse tailings that form the upper slope of the reservoir. Cyclic triaxial tests and cyclic direct shear tests (CDSS) were also carried to assess the dynamic properties of the tailings materials.

3 SEISMICITY AT THE OTAPARA DAM SITE

3.1 Seismic classification

According to the Global Industry Standard on Tailing Management Methodology (GISTM, 2020), the Otapara tailings dam has a potentially significant risk that should consider a 1000-year return period (T_r) for the design earthquake.

3.2 Probabilistic Seismic Hazard Assessment (PSHA)

The PSHA was investigated using the methodology proposed by Cornell (1968) implemented in the software R-CRISIS (Ordaz et al., 2020). It was estimated the seismic hazard for a probability of exceeding 5% in 50 years, corresponding to a return period of 1000 years. The calculation of the peak ground acceleration (PGA) in the Otopara dam site was done using a regular mesh of 0.1º in longitude and latitude.

The identification and characterization of the seismogenic sources were taken from Aguilar et al. (2017). For subduction and continental earthquakes, some specific ground motion prediction equations (GMPEs) were selected and used in a logic tree framework, in order to reduce the epistemic uncertainties inherent in the seismicity models.

From the estimated seismic risk curves for different structural periods, it was possible to obtain the Uniform Hazard Spectra (UHS) that presents acceleration values in different structural periods for the same annual exceedance probability considering an exposure time of 50 years of the structure (Figure 3).

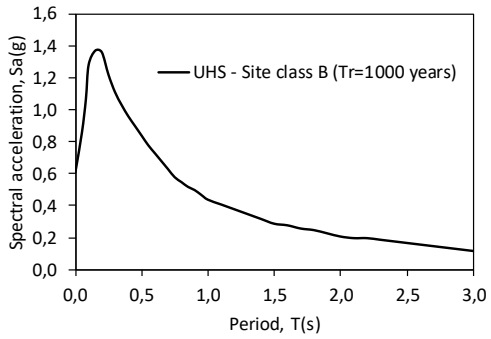

Figure 3. Spectral acceleration response for 1000-year return period.

The seismic hazard disaggregation (Figure 4) also provides a useful insight into the main sources contributing to the hazard at the Otapara dam site. The interface earthquake of magnitude 6.3 M_w at 65 km distance generates the greatest contribution, but it is also important to notice that there is another main contribution from a 5.4 M_w intraplate earthquake at a distance of 65 km.

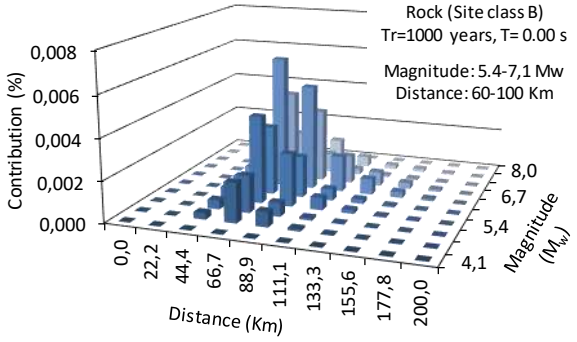

Figure 4. Disaggregation of probabilistic seismic hazard (PGA) for 5% probability of exceedance in 50 years.

3.3 Design Earthquakes

Considering the results obtained in the disaggregation procedure, seismic records with similar spectral content, magnitude, epicentral distance and focal rupture mechanism were selected. In this investigation, the Lomas (2018), Atico (2001) and Lima (1974) seismic records were chosen for seismic modeling (Table 1).

Table 1. Earthquakes considered for the present analysis.

Earthquake	Lomas	Atico	Lima
Date	Jan 14, 2018	Jun 23, 2001	Oct 03, 1974
Magnitude (M_w)	7.1	8.2	7.4
Rupture mechanism	Subduction interface	Subduction interface	Subduction interface
Depth (km)	27	33	13
Station	Caraveli (IGP)	Moquegua (CISMID)	Lima (PRQ)
Duration (sec)	115.01	198.92	97.96
Acceleration (g)	0.26	0.30	0.20

The spectral matching method (Al Atik & Abrahamson, 2010) was used to generate the artificial accelerograms whose response spectra should be consistent with the target spectrum obtained in the PSHA. Figure 5 shows the response spectra (before and after spectral matching) while Figure 6 presents the artificial accelerograms for each one of the earthquakes considered in this analysis.

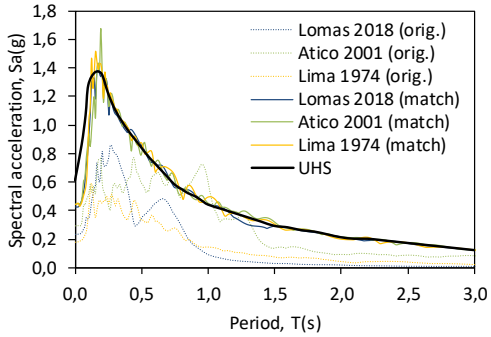

Figure 5. Response spectra before and after spectral matching.

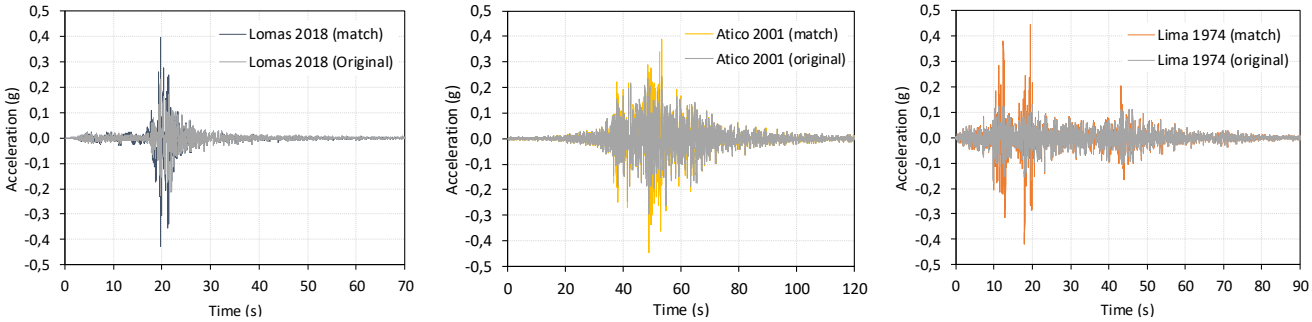

(a) (b) (c)

Figure 6. Acceleration histories before and after spectral matching for the three selected earthquakes (a) Lomas 2018; (b) Atico 2001; (c) Lima 1974.

4 SEISMIC RESPONSE OF THE OTAPARA TAILING DAM

The numerical results from finite element analysis were compared with the values of safety factor against liquefaction determined by the simplified stress-based methods. In the numerical model, the mechanical behaviour of the tailing materials was simulated with the PM4Sand (Boulanger and Ziotopoulou, 2015) and the PM4Silt (Boulanger and Ziotopoulou, 2018) elastoplastic constitutive models, capable of estimating the dynamic liquefaction triggering and softening of materials when subjected to cyclic loading.

4.1 Cross-section geometry

The geometry of the representative cross-section of the dam is shown in Figure 7, indicating the occurrence of bedrock (R), embankment (E), alluvial deposit (AD) and tailings (T0, T1, T2, T3, T4, T5, T6).

According to Lysmer and Kuhlemeyer (1973) recommendations, a suitable maximum mesh spacing is usually determined by considering a tenth of the minimum relevant wavelength (or highest frequency f_{max}) in the input signal. The finite element size for the tailings was prescribed as 2.0 m while for the other materials the values ranged from 5.0 m to 35.0 m.

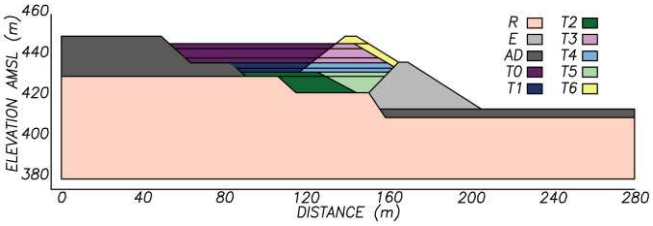

Figure 7. Materials in the Otopara dam cross-section.

4.2 Material Properties

Based on field investigation, laboratory tests and correlations from literature, the geotechnical parameters for all materials were obtained. The linear elastic model was used to mechanically represent the bedrock behaviour (E = 13,500 MPa, ν = 0.2), while the elastoplastic HSM model (Schanz, 1999) was chosen to simulate the response of the embankment and the alluvial deposit (Table 2), and the PM4Sand and PM4Silt models were used for the tailings (Table 3 and 4).

Table 2. Parameters used for the seismic analysis of non-liquefiable materials.

Material	SUCS	γ_{sat} (kN/m^3)	E_{50}^{ref} (kPa)	E_{oed}^{ref} (kPa)	E_{ur}^{ref} (kPa)	M (-)	c' (kPa)	ϕ' (°)	G_0^{ref} (kPa)	$\gamma_{0.7}$ (-)
E	GM	21.0	60,000	60,000	180,000	0.5	10	37.0	239,000	0.0001
AD	GM	20.0	45,000	45,000	135,000	0.5	5	37.0	239,000	0.0002

Table 3. PM4Sand parameters for the tailings layers

Material	SUCS	γ_{unsat}	γ_{sat}	D_r	G_o	h_{po}
T0	SM	16.5	20.0	0.40	524	0.27
T1	SM	16.5	20.0	0.40	524	0.27
T3	SM	16.5	20.0	0.40	524	0.20
T4	SM	17.0	20.0	0.60	729	0.11
T5	SM	17.0	20.0	0.65	574	0.90
T6	SM	19.0	20.0	0.80	944	1.00

Table 4. PM4Silt parameters for tailings layers with softening behaviour

Material	SUCS	γ_{unsat}	γ_{sat}	$S_{u,ratio}$	G_o	h_{po}
T2	ML	19.0	20.0	0.30	400	6.8

An elastic analysis was previously performed to determine Rayleigh's damping coefficients in the materials that make up the dam, although for the tailings only hysteretic damping was considered. Table 5 shows the values of the damping coefficients α and β.

Table 5. Rayleigh damping for seismic analysis.

Material	α	β
E, AD, R	0.29	0.0048

4.3 Parameter calibration for cyclic models

The primary parameters for the PM4Sand and PM4Silt constitutive models are based on correlation of the relative density with SPT data. Specifically, the h_{po} parameter was calibrated using the Plaxis 2D Soil Test module, taking results from CDSS and cyclic triaxial tests on tailings samples carried out at different confinement stresses. Figure 8 shows the stress-strain response between laboratory results (black curves) and the calibrated constitutive model (PM4Sand) for a sample from tailings T5. The same procedure was carried out for other samples, trying to approximate the calibrated cyclical response (blue curves) to the results obtained in the laboratory tests.

Figures 9 to 13 show the cyclical resistance curves. A data conversion from cyclic triaxial tests to CDSS single shear strain mode was performed following the procedure suggested by Cappellaro et al. (2017).

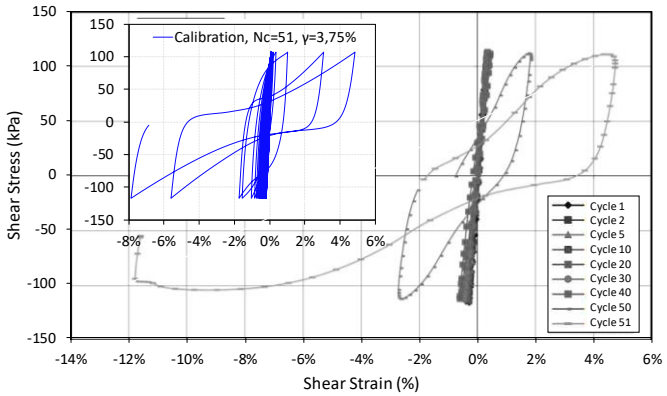

Figure 8. Calibration of CDSS test carried out in sample from tailing T5.

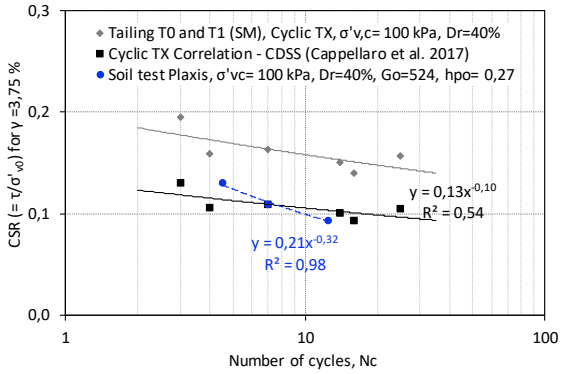

Figure 9. Cyclic resistance curves, calibration of samples from tailings T0 and T1.

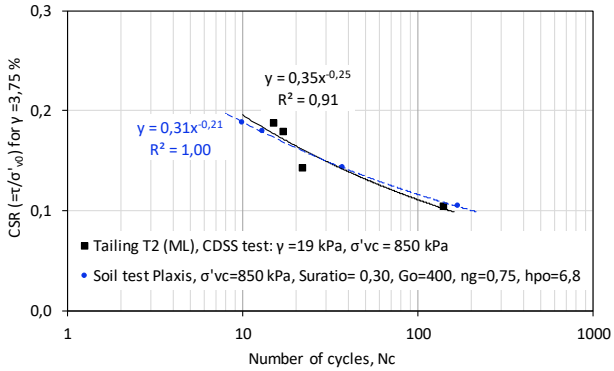

Figure 10. Cyclic resistance curves, calibration of sample from tailing T2.

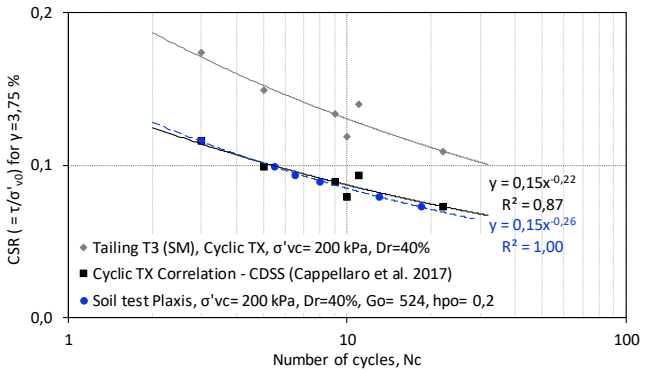

Figure 11. Cyclic resistance curves, calibration of sample from tailing T3.

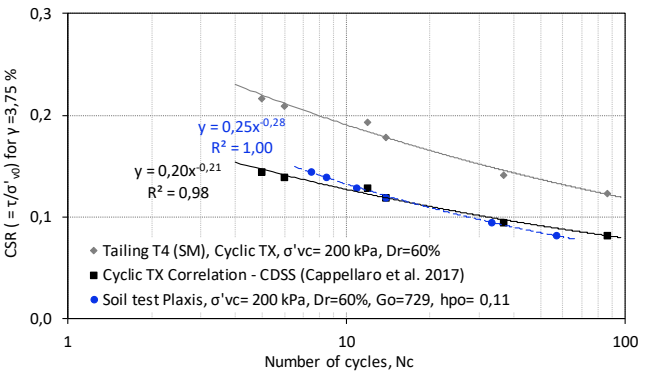

Figure 12. Cyclic resistance curves, calibration of sample from tailing T4.

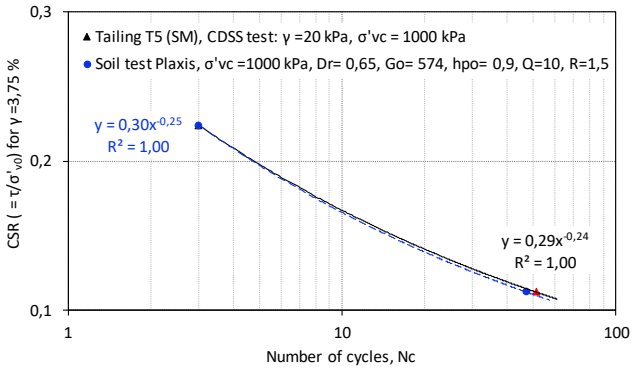

Figure 13. Cyclic resistance curves, calibration of sample from tailing T5.

4.4 Permanent Displacements

The total permanent displacements induced by the Lomas (2018), Atico (2001) and Lima (1974) earthquakes may be seen in Figure 14.

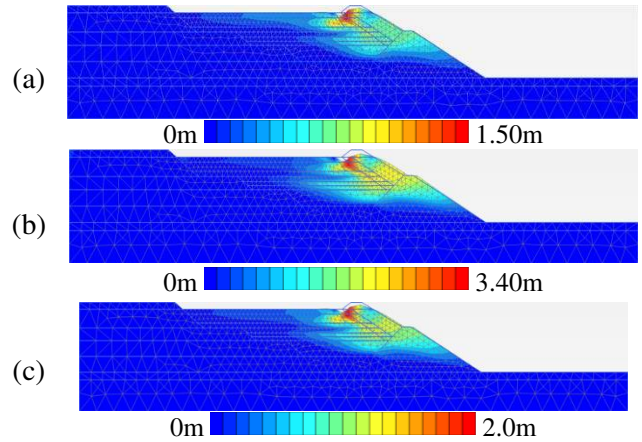

Figure 14. Total permanent displacements provoked by (a) Lomas 2018; (b) Atico 2001; (c) Lima 1974 earthquakes.

4.5 Distribution of pore pressure ratio (r_u)

In this research, it was used the definition of the pore pressure raio r_u given by Beaty and Byrne (2011):

$$r_u = 1 - \left(\frac{\sigma'_v}{\sigma'_{vo}}\right) \qquad (1)$$

where σ'_v is the current effective vertical stress and σ'_{v0} represents the initial effective vertical stress. Figure 15 shows the r_u distribution immediately after the seismic excitation duration, where may be seen that large regions of the tailings reservoir suffer dynamic liquefaction with $r_u = 1$ for all 3 earthquakes considered in the analysis.

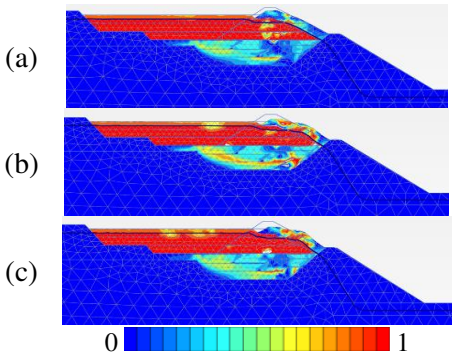

Figure 15. Distribution of pore pressure ratio (r_u) immediately after the (a) Lomas 2018; (b) Atico 2001; (c) Lima 1974 earthquakes.

5 CONCLUSIONS

According to the GISTM (2020) methodology, the Otapara tailings dam was classified as a structure of significant potential risk for dynamic liquefaction, under earthquakes with a return period of 1000 years. The design earthquakes were generated with basis on a probabilistic seismic hazard assessment for the Otapara dam, considering GMPEs for class B (rock). The Lomas (2018), Atico (2001) and Lima (1974) seismic records were chosen for seismic modeling considering their magnitudes, epicentral distances, focal rupture mechanisms and frequency contents.

Simplified stress-based methods were initially used to estimate the potential of liquefaction triggering through deterministic and probabilistic approaches. The results were confirmed by finite element analysis considering the PM4Sand and PM4Silt elastoplastic models to represent the seismic behaviour of the tailings materials.

The earthquakes provoked maximum permanent displacements between 1.5 to 3.4 m and high pore pressures in the tailings reservoir, leading to dynamic liquefaction, as indicated by the pore pressure ratio $r_u = 1$ in large regions of the Otopara dam.

ACKNOWLEDGEMENTS

To the National Council for Scientific and Technological Development (CNPq) of Brazil for the scholarships granted to the two first authors.

REFERENCES

Aguilar, Z., Roncal, M., Piedra, R. 2017. Probabilistic Seismic Hazard Assessment in the Peruvian Territory, 16 WCEE – *World Conference on Earthquake, 1-10.*

Al Atik, L., & Abrahamson, N. 2010. An improved method for nonstationary spectral matching. *Earthquake spectra*, 26(3), 601-617.

American Society of Civil Engineers – ASCE. 2017. Minimum Design Loads and Associated Criteria for Buildings and Other Structures. *ASCE Standard ASCE/SEI 7-16*. Reston, Virginia.

Barrero, A. R., Taiebat, M., & Dafalias, Y. F. 2020. Modeling cyclic shearing of sands in the semifluidized state. *International Journal for Numerical and Analytical Methods in Geomechanics*, 44(3), 371-388.

Beaty, M., & Byrne, P. M. 1998. An effective stress model for pedicting liquefaction behaviour of sand. *Geotechnical Earthquake Engineering and Soil Dynamics III* (pp. 766-777). ASCE.

Beaty, M. H.; Byrne, P. M. 2011. UBCSAND Constitutive Model version 904aR. *Itasca UDM Web Site*, 69.

Boulanger, R. W.; Ziotopoulou, K. 2015. PM4Sand (version 3): A sand plasticity model for earthquake engineering applications. *Report No. UCD/CGM-15/01*, Center for Geotechnical Modeling, Department of Civil and Environmental Engineering, University of California, Davis, Calif.

Boulanger, R. W.; Ziotopoulou, K. 2018. PM4Silt (version 1): A silt plasticity model for earthquake engineering applications. *Report No. UCD/CGM-18/01*, Center for Geotechnical Modeling, Department of Civil and Environmental Engineering, University of California, Davis, CA, 108 pp.

Cappellaro, C., Cubrinovski, M., Chiaro, G., Stringer, M. E., Bray, J. D.; Riemer, M. F. 2017. Undrained cyclic direct simple shear testing of Christchurch sandy soils. *20th NZGS Geotechnical Symposium* (pp. 1-8).

Cornell, C. A. 1968. Engineering seismic risk analysis. *Bulletin of the Seismological Society of America*, 58(5), 1583-1606.

Dafalias, Y. F., & Manzari, M. T. 2004. Simple plasticity sand model accounting for fabric change effects. *Journal of Engineering Mechanics*, 130(6), 622-634.

Dafalias, Y. F., & Taiebat, M. 2016. SANISAND-Z: zero elastic range sand plasticity model. *Géotechnique*, 66(12), 999-1013.

GISTM Global Industry Standard on Tailings Management 2020. *International Council on Mining and Metals* - ICMM.

Kuhlemeyer, R.L; Lysmer, J. 1973. Finite element accuracy for wave propagation problems, *Journal of the Soil Mechanics and Foundations Division*, vol. 99(5), p. 421-427.

Ordaz, M., & Salgado-Gálvez, M. A. (2020). R-CRISIS v20 Validation and verification document. Mexico City: *ERN Technical Report*.

Papadimitriou, A. G., Chaloulos, Y. K., & Dafalias, Y. F. 2019. A fabric-based sand plasticity model with reversal surfaces within anisotropic critical state theory. *Acta Geotechnica*, 14(2), 253-277.

Petalas, A. L., Dafalias, Y. F., & Papadimitriou, A. G. 2019. SANISAND-FN: An evolving fabric-based sand model accounting for stress principal axes rotation. *International Journal for Numerical and Analytical Methods in Geomechanics*, 43(1), 97-123.

Petalas, A. L., Dafalias, Y. F., & Papadimitriou, A. G. 2020. SANISAND-F: Sand constitutive model with evolving fabric anisotropy. *International Journal of Solids and Structures*, 188, 12-31.

Petalas, A., & Galavi, V. 2013. Plaxis liquefaction model UBC3D-PLM. *Plaxis Report*.

Schanz, T. 1999. Formulation and verification of the Hardening-Soil Model. RBJ Brinkgreve, *Beyond 2000 - Computational Geotechnics*, 281-290.

Taiebat, M., & Dafalias, Y. F. 2008. SANISAND: Simple anisotropic sand plasticity model. *International Journal for Numerical and Analytical Methods in Geomechanics*, 32(8), 915-948.

Tsegaye, A. 2010. Plaxis liquefaction model. external report. *PLAXIS knowledge base*.